Acta Pharmaceutica Sinica B 2025;15(4):1912−1921

Chinese Pharmaceutical Association
Institute of Materia Medica, Chinese Academy of Medical Sciences

Acta Pharmaceutica Sinica B

www.elsevier.com/locate/apsb
www.sciencedirect.com

TOOLS

Construction and application of a large capacity VNAR library from the whitespotted bamboo shark (*Chiloscyllium playgiosum*)

Hao Li[a,†], Litong Liu[b,†], Xinyi Kang[c,†], Chuan-Wei Chen[a,†], Mengran Wang[d,†], Shaoqin Fu[e], Qingtong Zhou[a,c], Bo Zhao[d], Dehua Yang[a], Ming-Wei Wang[a,c,f,g,*]

[a]*Research Center for Deepsea Bioresources, Sanya 572025, China*
[b]*Shanghai Institute of Infectious Disease and Biosecurity, Fudan University, Shanghai 200032, China*
[c]*Department of Pharmacology, School of Basic Medical Sciences, Fudan University, Shanghai 200032, China*
[d]*School of Pharmaceutical Sciences, Shanghai Jiao Tong University, Shanghai 200240, China*
[e]*Yazhou Bay Agricultural and Fishery Development Co., Ltd., Sanya 572000, China*
[f]*Research Center for Medicinal Structural Biology, National Research Center for Translational Medicine at Shanghai, State Key Laboratory of Medical Genomics, Ruijin Hospital, Shanghai Jiao Tong University School of Medicine, Shanghai 200025, China*
[g]*Engineering Research Center of Tropical Medicine Innovation and Transformation of Ministry of Education, School of Pharmacy, Hainan Medical University, Haikou 570228, China*

Received 15 September 2024; received in revised form 9 December 2024; accepted 9 January 2025

KEY WORDS

Shark;
Chiloscyllium playgiosum;
VNAR;
Immunization;
Phage display;
HSA;
TFEB

Abstract Fifty whitespotted bamboo sharks (*Chiloscyllium playgiosum*) of both sexes were used to establish a large capacity variable domain of the new antigen receptor (VNAR) library with a total capacity of over 10^9 colony-forming units (CFU). It was applied to screen VNARs against human serum albumin (HSA) and human transcription factor EB (TFEB), respectively. Meanwhile, VNAR libraries specific to HSA and TFEB with capacities above 10^8 CFU were obtained following conventional immunization. These two approaches were systematically studied in terms of VNAR yield and composition. By comparing the VNAR sequences obtained from naïve and antigen-immunized libraries, we found that the complementary-determining region 3 (CDR3) of the former differs in composition from that of the latter. It shares a higher degree of homology with the naïve library. Meanwhile, the binding efficiency assessed by ELISA is also different between the naïve and antigen-immunized libraries. The binding

*Corresponding author.
E-mail address: mwwang@simm.ac.cn (Ming-Wei Wang).
[†]These authors made equal contributions to this work.
Peer review under the responsibility of Chinese Pharmaceutical Association and Institute of Materia Medica, Chinese Academy of Medical Sciences.

https://doi.org/10.1016/j.apsb.2025.02.012

of VNARs from the TFEB-immunized library appeared to surpass that observed with the naïve libraries, whereas the performance of VNARs from the HSA-immunized library indicated that both the immunized and naïve libraries for HSA had positive binding responses in polyclonal and monoclonal ELISA. The results are useful to develop novel diagnostic and therapeutic products based on shark VNARs.

1. Introduction

The therapeutic antibody market has experienced unprecedented growth in recent decades[1,2], with global sales exceeding $232 billion in 2023. However, the limitations of traditional immunoglobulin G (IgG) antibodies, due to their large molecular weight (approximately 150 kDa), have become increasingly evident[3]. Single-domain antibodies (sdAbs) have emerged as a promising next-generation therapeutic platform, offering distinctive advantages in terms of molecular weight, stability, and expression systems[4-6]. These molecules demonstrate not only high binding affinity but also superior accessibility to sterically hindered epitopes[7] that are typically inaccessible by conventional IgGs. Furthermore, their small size facilitates enhanced tissue penetration, including the ability to cross biological barriers such as the blood−brain barrier (BBB)[8-10], eye tissue[11] and solid tumors[5]. Currently, the most extensively investigated sdAbs are the variable regions of heavy-chain antibodies (VHHs) derived from camelids and the variable new antigen receptors (VNAR) from cartilaginous fish[12]. The discovery of a naturally occurring heavy-chain antibody family (HCAbs) lacking light chains in the humoral immune system of camelids in 1993 marked a significant breakthrough in antibody research[13]. A parallel discovery in 1995 identified an immunoglobulin (Ig)-based novel antigen receptor (IgNAR) in the nurse shark (*Ginglymostoma cirratum*) serum[14]. The antigen-binding variable domains of these unique antibodies, termed VHH and VNAR, respectively, have molecular weights of 11−15 kDa[15,16]. The evolutionary divergence of the shark immune system has endowed VNAR with distinct structural characteristics[17]. Each VNAR contains only two complementarity determining regions (CDR1 and CDR3) and two additional hypervariable loops (HV2 and HV4)[18], resulting in an even more condensed molecular weight compared to VHHs. Notably, the absence of CDR2 contributes to enhanced sequence, length, and conformational diversity within the VNAR CDR3 region[19,20], which plays a crucial role in antigen recognition specificity. The structural stability of VNAR is further enhanced by intramolecular disulfide bonds and hydrogen bonds that stabilize the CDR loops[18,19]. Additionally, the evolutionary adaptation to high urea concentrations in shark blood, necessary for osmotic regulation in marine environments, has contributed to the exceptional stability of VNAR molecules under extreme conditions[21].

Despite these compelling advantages, the widespread application of VNARs has been constrained by technical challenges in obtaining high-quality molecules, emphasizing the critical importance of establishing suitable model organisms for VNAR research and development. Early studies on sdAb have predominantly focused on camelids, primarily due to their manageable husbandry requirements compared to sharks[22]. While nurse sharks served as the initial model for IgNAR studies, research utilizing cartilaginous fish has been limited by various factors affecting most shark species suitable for VNAR generation, including their endangered status, large size, prolonged maturation time, aggressive nature, and challenges in laboratory maintenance[23]. Recent genomic studies, however, have identified the whitespotted bamboo shark (*Chiloscyllium plagiosum*) as a model organism, being the first shark species documented to possess a complete chromosomal configuration of all IgNAR clusters[5,10,12,24-26], capable of generating high-affinity VNARs following systematic immunization protocols[27-29]. The whitespotted bamboo shark's characteristics as a small, benthic species with rapid growth and adaptability to laboratory conditions make it particularly suitable for experimental immunology research[24]. This species presents a unique opportunity to advance our understanding of VNAR biology and development[12].

In this study, we employed the whitespotted bamboo shark as a model organism to establish both naïve and antigen-specific immunized libraries, enabling systematic evaluation of screening outcomes against diverse antigens. Through comparative analysis, we investigated the screening efficacy across different library formats. Our findings not only validate the whitespotted bamboo shark as a viable model organism for VNAR research but also provide critical insights into optimizing VNAR screening strategies against various antigen types.

2. Methods

2.1. Animals

Wild-caught healthy adult whitespotted bamboo sharks (*Chiloscyllium playgiosum*) from the coastal area of Sanya, Hainan, China, were utilized in this study. These animals were maintained at 23 °C in sterilized natural seawater in pools of Yazhou Bay Agriculture and Aquaculture Development Co., Ltd. and used according to the guidelines set forth by the Institutional Animal Care and Use Committee. This study has been approved by the Institutional Animal Care and Use Committee of the Sanya Yazhou Bay Agricultural and Aquaculture Development Co., Ltd. (SYAA), Protocol No. SYAA-202302001.

2.2. Immunization

Individual sharks, approximately 60−70 cm in length and weighing 0.5−1 kg, were immunized with human serum albumin (HSA, MW = 67 kDa; Sigma−Aldrich, MO, USA) or full-length human transcription factor EB [TFEB, MW = 52.8 kDa; expressed in *E. coli* BL21 (DE3) and purified with Ni + His Trap, Anhui General Biol Co., Ltd.] by subcutaneous injection into the abdominal posterior fins (right or left side). Each shark received 8 injections (100 μg in Montanide ISA-201, SEPPIC, Paris, France) at two-week intervals. Inoculation emulsions were prepared at an antigen-to-adjuvant ratio of 1:1 (*v*:*v*). Anesthesia was performed with MS-222 before immunization, blood collection, and dissection.

2.3. *Blood collection*

Whole blood samples (5 mL) were collected from the caudal vein of adult sharks and centrifuged at 30 × *g* for 5 min at room temperature (RT) to separate buffy coat containing peripheral blood mononuclear cells (PBMCs) and plasma. The cell pellets were resuspended in TRIzol (ThermoFisher Scientific, Waltham, MA, USA) before storage at −80 °C (Fig. 1).

2.4. *Naïve VNAR library*

Target RNA was extracted from the PBMCs of 50 healthy adult whitespotted bamboo sharks (1:1 male-to-female ratio). Total RNA was obtained by lysis solution and phenol−chloroform centrifugation, followed by treatment with DNase to remove possible contamination by genomic DNA. Random primers and the extracted RNA were used as templates to synthesize cDNA with reverse transcriptase which was purified by RevertAid reverse transcriptase kit (Takara, Otsu, Japan) thereafter.

The above reverse-transcribed cDNA library was subsequently used to design primers for the conserved regions Framework Region 1 (FR1) and FR4 flanking the VNAR region, and NotI and XbaI double restriction enzyme sites on the pComb3 phagemid vector (Addgene, Watertown, MA, USA). Polymerase chain reaction (PCR) was applied to amplify antibody genes (Fig. 2), yielding products of 300−500 base pairs (bp), which were subsequently purified. The gene fragments and the vectors were digested overnight at 37 °C using NotI and XbaI to facilitate ligation of the antibody genes. Following electrotransformation of the VNAR pCmob3 recombinant plasmid into *E. coli* SS320 competent cells (Lucigen, Beijing, China) under 180 V, 1.8 kV, and 25 μF, 1 mL SOC medium (Lucigen, Wisconsin, USA) was introduced with shaking at 37 °C for 1 h. Gradient dilution was made with 10 μL bacterial solution to determine the library capacity. The remaining bacterial solution was evenly spread on a Luria−Bertani (LB) agar plate (Sangon Biotech, Shanghai, China) with ampicillin and cultured overnight at 37 °C prior to extraction into a plasmid the next day, which was then electroporated into SS320 competent cells and verified by DNA sequencing to determine the diversity and integrity of the library (stored at −80 °C).

2.5. *Antigen-immunized VNAR library*

cDNA from PBMCs of the sharks previously inoculated with different antigens was used to amplify VNAR genes as described in the literature[30]. Specifically, cDNA fragments were amplified using a gradient annealing program ranging from 60 to 65 °C. The polymerase chain reaction (PCR) products were analyzed using 2% agarose gel electrophoresis, and the target fragments were extracted and purified. The purified PCR products were then digested with the restriction enzyme SfiI (New England Biolabs, Beverly, MA, USA) followed by ligation into the pComb3 vector using T4 DNA ligase (New England Biolabs) at 16 °C for 24 h. The ligation products were purified and transformed into electrocompetent *E. coli* TG1 cells (Lucigen, Wisconsin, USA) by electroporation under the preset conditions of 1.8 kV, 25 μF, and 200 Ω. After electroporation, the cells were immediately transferred into SOC medium (Lucigen, Wisconsin, USA) and incubated at 37 °C with shaking at 250 rpm for 1 h to allow full recovery.

Following recovery, the bacterial suspension (10 μL) was transferred to a sterile Eppendorf tube, while the remaining suspension was added to 2YT liquid medium (Sangon Biotech, Shanghai, China) and incubated at 37 °C with shaking at 250 rpm. When the bacterial culture reached an OD_{600} value of 0.6−0.8, a helper phage M13 (New England Biolabs), at a multiplicity of infection (MOI) of 10:1 (phage to bacteria) was added, followed by infection at 37 °C for 1 h. The bacterial cells were then collected by centrifugation and resuspended in 2YT medium containing 100 μg/mL ampicillin and 50 μg/mL kanamycin and incubated at 30 °C with shaking at 220 rpm for 14−16 h. The following day, the bacterial culture was centrifuged at 640 × *g* for 10 min, and the supernatant was collected. One-fourth volume of 20% PEG8000-NaCl solution (2.5 mol/L NaCl) (Sangon Biotech, Shanghai, China) was added to the

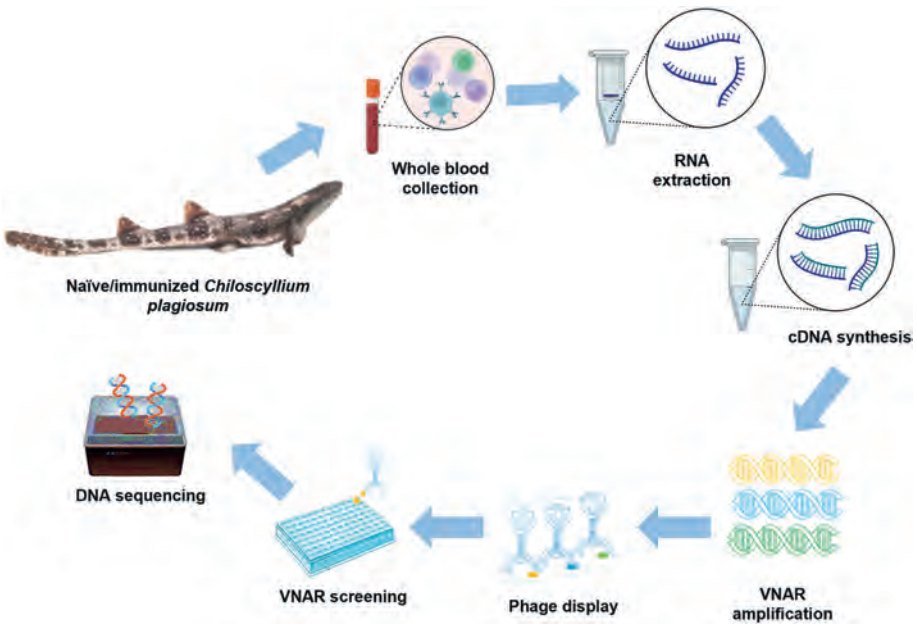

Figure 1 Variable domain of the new antigen receptor (VNAR) library construction and screening.

Name	Primer sequence	Reagent	Volume (μL)	Temperature (℃)	Time
VNAR1	F'gttgaacaaacaccgacaac	F	2	95 ℃	30 s
	R'ttcacagtcagaatggtg	R	2	95 ℃	15 s
VNAR2	F'gttgaccaaacaccgagaac	cDNA	1	56 ℃	15 s 30×
	R'tttcactgccagaaaagtg	Taq	25	72 ℃	60 s
VNAR3	F' gtggaccaaacaccgaaaac	H_2O	20	72 ℃	5 min
	R'tttcacagtcagaatggtg	System	50	4 ℃	30 min
VNAR4	F'attgatcaaaaaccgagatc				
	R'gttcacagtcagaacggtg				

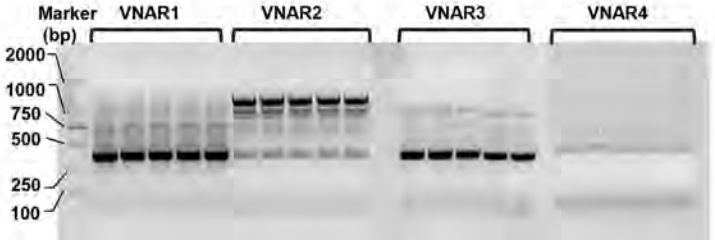

Figure 2 Construction and sequences of shark VNAR libraries. Primers and PCR conditions used in constructing naïve VNAR libraries (VNAR1 and VNAR2).

supernatant to precipitate the recombinant phage. The mixture was centrifuged at 640 × *g* for 20 min at 4 °C, and the supernatant was discarded. The phage pellet was resuspended in PBS containing 50% glycerol, and the phage titer was determined by measuring the absorbance at 280 nm using a spectrophotometer (OD_{280} = 2.33 × 10^{12} pfu/mL). This constituted the phage VNAR library, which was aliquoted and stored at −80 °C.

2.6. *Phage display screening and panning*

2.6.1. *Solid phase*

The library was thawed on ice and recombinant phages were precipitated by adding one-fourth volume of 20% PEG8000-NaCl solution (2.5 mol/L NaCl). For the first round of selection, microtiter plates were coated with antigen (10 μg/mL in PBS) and incubated overnight at 4 °C. Upon removal of excess antigens, the plates were blocked by PBS containing 5% skim milk powder (MPBS, *w/v*) at 37 °C for 1 h and eluted with 0.05% PBST (Solarbio Life Sciences, Beijing, China) thereafter. Phage particles (approximately 1000 times the phage reservoir capacity) were introduced to the plates for binding at 37 °C for 1 h. The unbound phage particles were washed away with 0.05% PBST. For subsequent panning rounds, antigen concentrations were decreased to 1−5 μg/mL allowing sufficient elution to enrich antigen-specific phages.

2.6.2. *Liquid phase*

The screening was conducted as previously described[31]. The library was thawed on ice and recombinant phages were precipitated by adding one-fourth volume of 20% PEG8000-NaCl solution (2.5 mol/L NaCl). After discarding the supernatant, the phage pellet was resuspended in PBS, blocked by 3% MPBS (*w/v*), and incubated with biotinylated antigen (ACRO Biosystems, Beijing, China; 5, 3, 2, and 1 μg for the first, second, third and fourth rounds, respectively) at RT on a rotary mixer for 0.5 h. Streptavidin-coated magnetic beads (Sigma−Aldrich) were then added and incubated for 1.5 h. Upon removal of the supernatant, the mixture was placed on a magnetic stand for washing with 0.05% PBST to discard unbound or nonspecifically bound phages. The phages bound to the magnetic beads were used to infect logarithmic-phase TG1 cells by incubation at 37 °C for 45 min without shaking. A 20 μL aliquot of the infected bacterial suspension was serially diluted 10^3-, 10^4-, and 10^5-fold, and 50 μL of each dilution was plated onto 2YT agar plates. The plates were incubated overnight at 30 °C to titrate the eluted phages. The remaining infected bacterial suspension was cultured in a 2YT medium containing 100 μg/mL ampicillin and 2% glucose at 37 °C with shaking at 250 rpm for 2 h. After the addition of approximately 10^{11} pfu of helper phage M13KO7, the culture was incubated at 37 °C for 45 min, followed by the removal of the magnetic beads. The TG1 bacteria cells were collected by centrifugation, resuspended in 2YT medium containing 100 μg/mL ampicillin and 50 μg/mL kanamycin, and incubated overnight at 30 °C with shaking at 220 rpm. The following day, the bacterial culture was centrifuged, and the supernatant was collected. One-fourth volume of 20% PEG8000-NaCl solution (2.5 mol/L NaCl) was added to the supernatant to precipitate recombinant phage VNARs, which were resuspended in PBS thereafter. This constituted the antigen-immunized VNAR library enriched in the first round, which was used for the next round of enrichment screening. This screening process was repeated four times in total, with each round utilizing 10^{12} phages. After four rounds of screening, polyclonal ELISA was performed on the phages obtained after each round to determine the degree of enrichment. Specifically, a 96-well ELISA plate was coated with 2 μg/mL of HSA and incubated overnight at 4 °C. It was then blocked by 3% MPBS (*w/v*) for 1 h. Subsequently, the supernatants from the library (10^{11} pfu phages) obtained after each round of screening were added to the HSA-coated plates and incubated at 37 °C for 1.5 h. Binding was detected using an HRP-anti-M13 antibody (Sino Biological, Beijing, China). Subsequently, the phage pool with the highest level of enrichment was selected for monoclonal ELISA identification. Specifically, the phages from the fourth round were employed to infect TG1 cells, which were subsequently plated on 2YT agar plates and incubated overnight at 30 °C. The following day, 200 μL of 2YT medium containing 100 μg/mL ampicillin was dispensed into each well of a round-bottom 96-well cell culture plate. Single colonies were randomly selected from the agar plates and inoculated into the wells, followed by incubation at 37 °C with shaking at 220 rpm for 6 h. Protein expression was induced by adding isopropyl β-D-1-thiogalactopyranoside [IPTG (Sigma−Aldrich)] to a final concentration of 1 mmol/L, with further incubation at 30 °C for

14−16 h. The bacterial cultures were then incubated with HSA, which had been precoated onto a 96-well ELISA plate, for 1.5 h. After washing the wells three times with PBST, an HRP-conjugated anti-Flag antibody (Sigma−Aldrich) was applied to detect positive monoclonal colonies.

2.7. Statistical analysis

The data analysis and graphing were performed by GraphPad Prism 8.0 software (GraphPad Software, San Diego, CA, USA). Binding kinetics and dissociation between TFEB and the antibody were monitored *via* surface plasmon resonance (SPR) on a Biacore™ 8K system (Cytiva, Marlborough, MA, USA) and analyzed with Biacore Insight Evaluation (software version 2.0.15.12933). At least three independent experiments were performed for TFEB, and representative or pooled data from repeated experiments are presented.

3. Results

3.1. General features of the VNAR libraries

VNAR residues were classified into four types based on the number and position of classical and non-classical cysteine residues within the domain. Four primer pairs were designed to construct VNAR libraries targeting the conserved regions of FR1 and FR4, located before and after the VNAR sequence, respectively[30]. These primers (Fig. 2) were used to construct the naïve VNAR libraries from pooled cDNA samples of 50 sharks under optimized experimental conditions. Excellent sequence diversity and integrity with a capacity of over 10^9 colony-forming units (CFU) was achieved (Supporting Information Fig. S1A) for both VNAR1 and VNAR2 libraries (Fig. S1B and S1C), thereby meeting the screening requirements[32]. The products (Fig. 3) with a length of 300−500 bp were subsequently used to construct libraries against HSA and TFEB, both with a capacity above 10^8 CFU. As shown in Supporting Information Fig. S2A and S2B, the insertion rate is approximately 90% and their amino acid sequences show different CDR3 colonies, indicating a high degree of diversity.

3.2. HSA versus TFEB screening

3.2.1. HSA-immunized library screening

The enrichment of phages after four rounds of screening was assessed using polyclonal ELISA. As demonstrated in Fig. 4A, a significant enrichment of VNAR was first noted during the third round of screening, with further substantial enrichment observed by the fourth round. Consequently, the fourth-round library was selected for monoclonal ELISA characterization (Fig. 4B). The significant fold change observed after screening indicates that certain molecules demonstrate potential binding activity to the target antigen.

The specific VNARs isolated through panning were subjected to DNA sequencing, revealing that six of the sequences were identical (data not shown). Subsequently, we selected five different enriched sequences from the sequencing results (data not shown), along with the sequences obtained from the screening, for expression and further validation.

3.2.2. TFEB-immunized library screening

Three rounds of panning were performed using TFEB as the antigen (Fig. 5A). Polyclonal ELISA results suggested an effective enrichment of TFEB-specific phages (Fig. 5B). Subsequently, 96 single colonies were randomly selected and evaluated *via* monoclonal ELISA (Fig. 5C). Based on the monoclonal ELISA results (OD_{450} values) and the sequencing data of the final enriched sequences, seven sequences with distinct CDR3 regions were selected for further validation (Supporting Information Fig. S3).

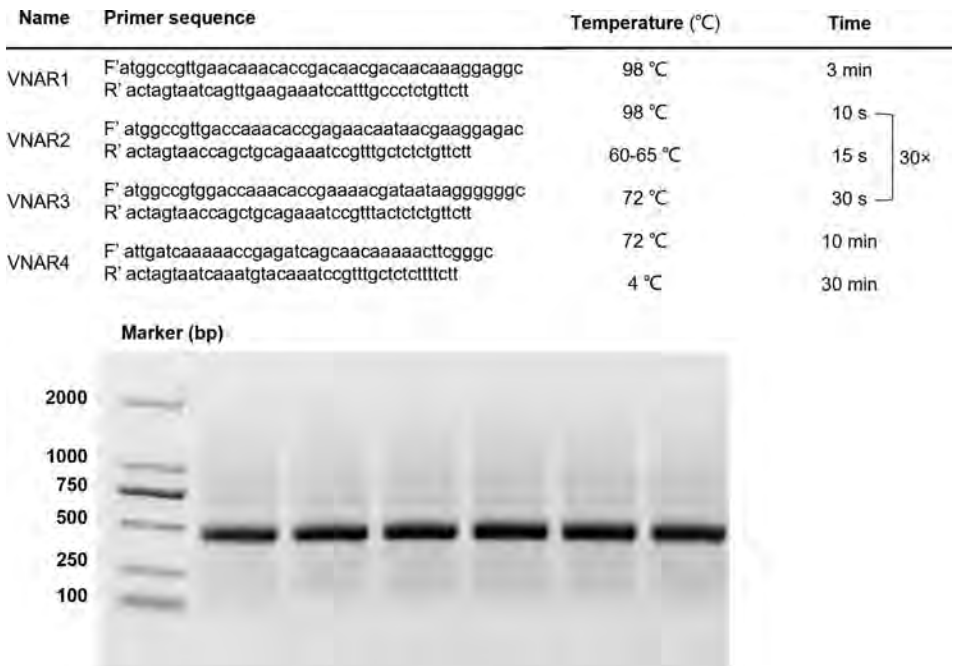

Figure 3 Primers and PCR conditions used in constructing human serum albumin (HSA)- and human transcription factor EB (TFEB)-immunized VNAR libraries.

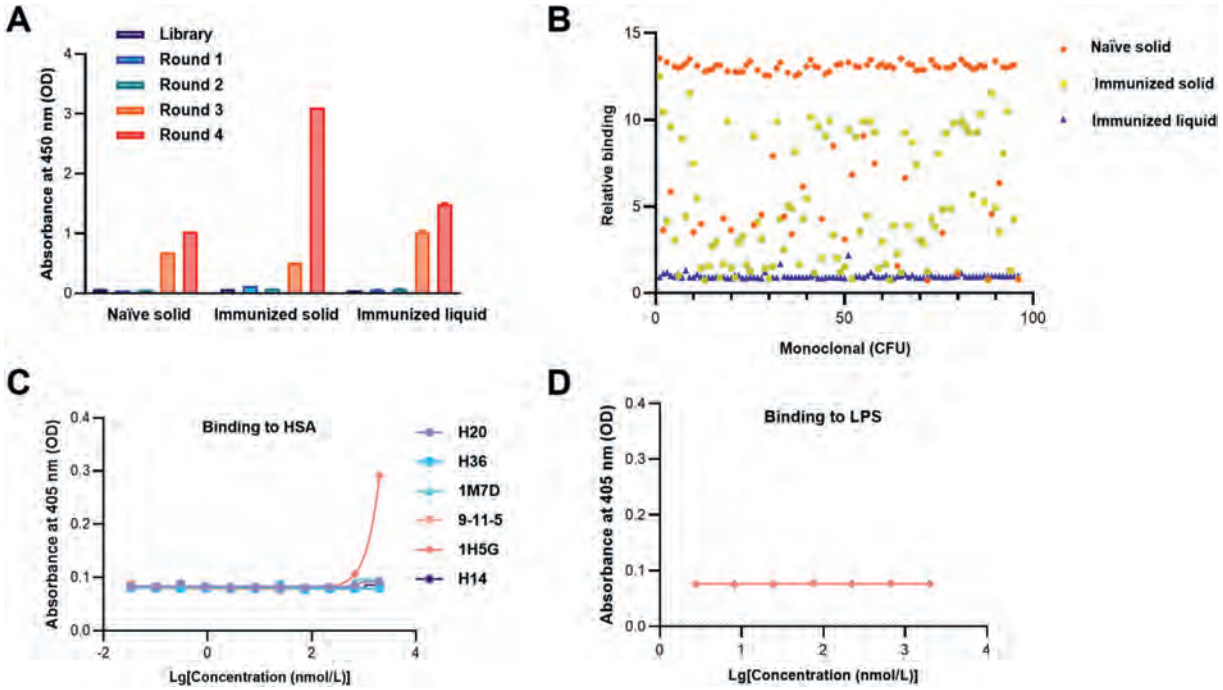

Figure 4 Panning and screening results of HSA-immunized VNAR library. (A) Polyclonal ELISA of HSA-immunized library. (B) Monoclonal ELISA of the HSA-immunized library (all relative binding values were normalized to the absorbance of the blank well). (C, D) Evaluation of VNAR affinity to HSA (C) and non-specific binding assessment (D) using ELISA. LPS, lipopolysaccharide.

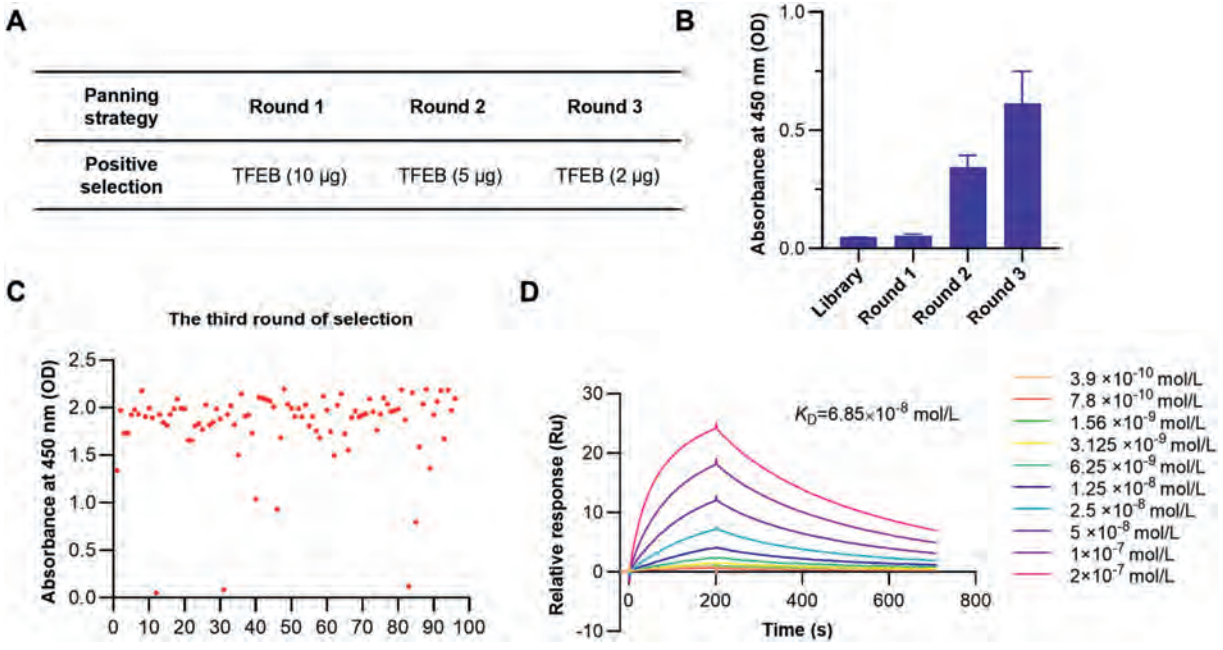

Figure 5 Panning and screening of TFEB-immunized library. (A) Panning conditions. (B) Polyclonal ELISA of TFEB-immunized library. (C) Monoclonal ELISA of TFEB-immunized library. (D) Surface plasmon resonance (SPR) sensorgram showing the binding affinity of VNAR T5.

3.2.3. Screening of the naïve library against TFEB

The naïve libraries (VNAR1 and VNAR2) were subjected to two rounds of panning using TFEB as the antigen (solid phase). Phage input and recovery in each round were statistically analyzed and single colonies were randomly selected for PCR to identify the full-length rate. The results showed a 10-fold difference in phage recovery between the experimental and control groups after the first round, with a 100% full-length rate (Fig. 6A). In the second round, due to the optimization of the experimental conditions, no significant difference in phage recovery was observed between the groups. PCR results showed that the full-length rate remained 100% (Fig. 6B), suggesting that enrichment of TFEB-specific VNARs likely occurred during the first round. Nine full-length sequences were identified from 20 randomly selected single

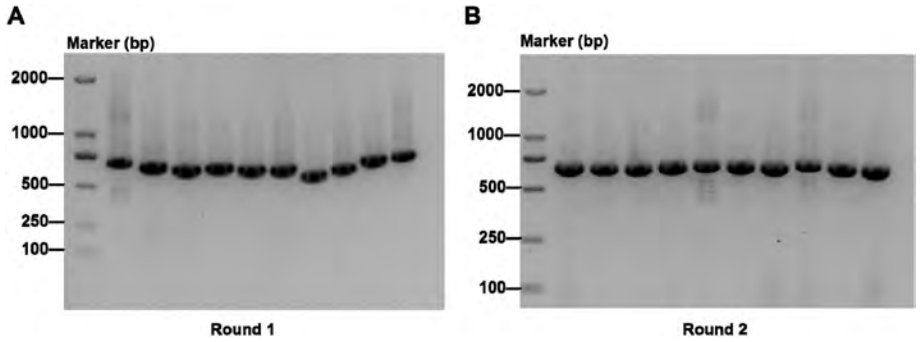

Figure 6 Colony PCR monitors the size of the phagemid insert fragments in the first (A) and second round (B) of screening.

colonies after the second round of panning. They were then resuscitated and cultured for identification of corresponding monoclonal phages by ELISA, yielding four monoclonal strains with high OD_{450} absorbance values (Fig. 7).

3.3. Naïve versus antigen-immunized library screening

In the naïve libraries, four full-length sequences were randomly selected and numbered as 5, 6, 17 and 19 (Fig. S3). Although, compared with the screening results of the TFEB-immunized library, there are multiple enriched VNAR sequences (Fig. S3), the CDR3 region of these four sequences did not show obvious enrichment. However, all showed ELISA reactivity. This implies that although the positive screening rate from the naïve library is low, it is still possible to obtain promising VNARs. Meanwhile, it also indicates that the TFEB-immunized library displays a higher efficiency in the screening of shark-derived nanobodies.

Four rounds of phage selection were conducted on the naïve and immune VNAR libraries using HSA as an antigen. Polyclonal ELISA results demonstrated that phage enrichment appeared in the fourth round. DNA sequencing was performed on the specific VNARs isolated by selection, revealing 7 sequences with distinct CDR3 regions in the HSA-immunized library and 19 in the naïve library. Sequence alignment (Supporting Information Fig. S4) showed that the CDR regions of the naïve VNAR1 library shared a high degree of homology with those from the HSA-immunized library, albeit the latter exhibits more residue variations.

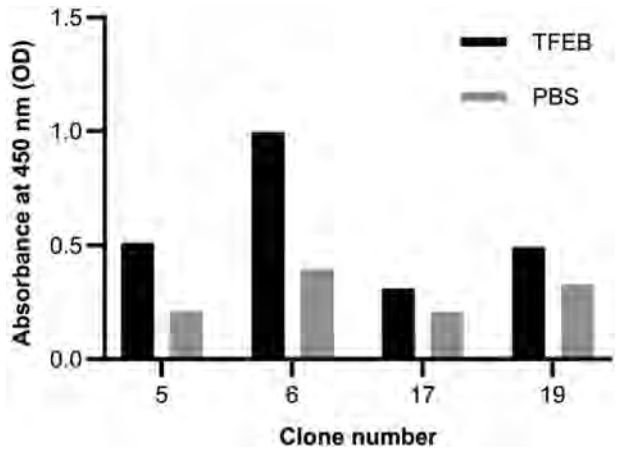

Figure 7 Identification of TFEB-specific phage clones with monoclonal ELISA.

Of interest is that all sequences obtained from screening of the HSA-immunized library belonged to VNAR1, while sequences from the naïve library yielded both VNAR1 and VNAR2, indicating that HSA could bind to multiple VNAR types, with a higher affinity for VNAR1. The results of polyclonal ELISA showed that the HSA-immunized library had a higher binding activity than that of the naïve. Monoclonal ELISA results indicated variable binding activities from immune and naïve libraries, suggesting that both are suitable for screening VNARs against HSA (Fig. 4A and B).

3.4. Solid versus and liquid phase screening

In the HSA-immunized library, six sequences were screened in liquid phase, of which three were enriched sequences, while seven sequences were screened in solid phase, of which only one was enriched sequence (Supporting Information Fig. S5). Solid phase screening uncovered sequences from both VNAR1 and VNAR2 *versus* only one using liquid phase. Sequences from the former displayed a high degree of homology.

3.5. Characterization of VNARs

As previously mentioned, seven sequences were identified from the TFEB-immunized library and four from the naïve libraries after panning. To characterize these sequences, the seven sequences were expressed using a cell-free expression system[33]. The production yields ranged from 2.5 to 5 mg/L (data not shown). SPR was performed to assess binding kinetics, and binding affinities were calculated from the kinetic parameters. Among them, only T5 exhibited a notable binding affinity to TFEB, with a K_D value of 6.85×10^{-8} mol/L (Fig. 5D).

Six VNARs against HSA were expressed and purified using a cell-free expression platform, yielding distinct target bands observed for all samples. The production yields ranged from 1 to 12 mg/L (data not shown). The binding affinities of these VNARs for HSA were subsequently evaluated by ELISA. As displayed in Fig. 4C and D, only the screened sequence demonstrated specific binding capability to the antigen. However, it was observed that its affinity for HSA was weak. This could be attributed to the fact that when we attempted to express the VNAR using a prokaryotic expression system, we observed either no target band or only a very faint target band. These results suggest that phage polyclonal and monoclonal ELISA evaluation systems may provide a more effective approach for screening VNARs from *Chiloscyllium plagiosum*, compared to the IPTG-induced periplasmic secretion method. This strategy could significantly enhance the likelihood of identifying high-quality candidate molecules.

4. Discussion

Large capacity antibody libraries[24] cover a wide range of antibody sequences and specificities, increasing the chances of discovering antibodies with specific functions, such as those against various disease-related antigens, toxins, or other molecular target[5,34]. In this study, we used 50 whitespotted bamboo sharks of both sexes to establish a large capacity VNAR library, containing two types, VNAR1 and VNAR2, with a combined capacity exceeding 10^9 CFU. It was applied to screen VNARs against HSA and TFEB, respectively. Meanwhile, VNAR libraries specific to HSA and TFEB with capacities above 10^8 CFU were obtained following a conventional immunization protocol. The two libraries were systemically compared in terms of VNAR yield and composition. HSA is a widely distributed serum protein[35] with multiple biological properties, and it shares homology across species[36,37]. Positive responses were detected from both the naïve and HSA-immunized library screenings, including enrichment in polyclonal ELISA and binding of monoclonal VNARs, indicating that both are suitable for the selection of nanobodies against HSA.

In contrast, TFEB is an intracellular transcription factor[38] that is not normally exposed to the immune system. Compared to the TFEB-immunized library, screening against the naïve library did not deliver an ideal yield. This can be explained by the fact that exogenous antigen stimulation typically induces stronger immune responses, leading to more specific VNAR sequences as reflected in our work. It appears that the suitability of naïve *versus* immune libraries is dependent on the nature of a given antigen. Generally, while immune libraries provide antibodies with better affinity and specificity caused by *in vivo* immune responses, the process of generating these libraries requires high-purity, concentrated antigen samples and the immunization of animals, making it more costly and time-consuming[39]. Furthermore, the success of immune libraries is influenced by several factors, including the nature of the antigen and the physical condition of the animals used[40,41]. In contrast, naïve libraries offer a simpler, more cost-effective alternative, bypassing the need for animal immunization[42]. Although antibodies derived from naïve libraries typically exhibit lower affinity, they provide broader specificities, making them suitable for a wider range of targets. Additionally, their affinity can be enhanced through subsequent affinity maturation or engineering steps, making naïve libraries a versatile tool for screening[31,43,44].

Evolutionary distance is often considered one of the key factors defining antigenicity[45]. Cartilaginous fish, which represent the first jawed vertebrate group[46], are also the oldest vertebrates with an adaptive immune system[47]. Due to the evolutionary divergence between mammals and sharks, this distance may enable sharks to generate high-affinity VNARs against conserved mammalian proteins like serum albumin[32,48]. Additionally, IgNAR undergoes iterative affinity maturation following immunization in sharks[49]. The first batches of antigen-specific IgNARs were isolated from nurse sharks immunized with lysozyme[50]. Comparison of sequences from hen egg-white lysozyme (HEL)-specific clones isolated from immunized phage libraries revealed the extent of somatic hypermutation and key residue changes that occurred during the affinity maturation process in sharks[51]. As expected, VNARs from immune libraries generally exhibit higher affinity and specificity than those from semi-synthetic or naïve libraries[52], a conclusion consistent with our results. However, for studies focusing on the selection of low-to moderate-affinity candidates, or when affinity maturation through engineering is the goal, naïve libraries are an excellent choice.

The CDR3 region plays a critical role in determining the affinity and specificity of antibody−antigen interactions[53-55]. Comparisons between the HSA-immunized and naïve libraries revealed that certain amino acids, such as serine, aspartic acid, and tyrosine, appeared more frequently in the CDR3 region of the naïve library. Previous researches have shown that the frequency of tyrosine is correlated with CDR3 length, suggesting conserved amino acid patterns may be crucial to the functionality of antibodies in both naïve and immune libraries[56,57]. Furthermore, structural stability in CDR3 is influenced by the presence of specific amino acids. Cysteines may form disulfide bonds within the antibody, contributing to antibody stability, while large hydrophobic residues like tryptophan help reduce water exposure, thus enhancing the internal stability of the antibody[58,59].

Regarding the construction and selection of naïve shark VNAR library, the present study revealed the diversity of distinct types of VNARs based on screening and panning of both naïve and immune libraries. Abundant diversity was found in VNAR1 and VNAR2, while VNAR3 and VNAR4 are conserved. This is consistent with the expression levels of different VNARs in sharks: VNAR1 > VNAR2 > VNAR3/VNAR4[30]. Therefore, it is recommended to prioritize VNAR1 and VNAR2 types when establishing a naïve library[60], particularly in the screening of nanobodies with significant diversity, allowing for enhanced "hit" efficiency and enrichment of more VNAR sequences of high quality[50]. In addition, ideal VNARs were identified even with a smaller naïve library (*e.g.*, 10^7 CFU)[61]. However, studies in camels suggest that VNARs having affinity comparable to monoclonal antibodies could be readily found in a large capacity naïve library (10^9 CFU)[62]. To further investigate this issue, we selected rat IgG as a new antigen[63], and an identical antibody sequence was unexpectedly identified through screening of both naïve and immune libraries that were exposed to different antigens, including rat IgG. As shown in Supporting Information Fig. S6, the VNAR sequences from four colonies (1-1 RAT, 1-7 RAT, 1-8 RAT, and 1-9 RAT) in the IgG (rat)-immunized VNAR library, and one colony (3-RAT naïve) from the naïve library, were identical. The results indicate that this sequence exhibited specific ELISA binding capacity towards the rat IgG. Previous studies have suggested that this antibody sequence may recognize a conserved epitope on the Fc domain[64], which enables binding to the conserved epitope. It is obvious that VNARs against a specific antigen could be retrieved from both immune and naïve libraries. Thus, the establishment of a large capacity and diverse naïve VNAR library, as shown here, would provide a solid foundation for future applications.

5. Conclusions

In conclusion, through a comparative analysis of screening outcomes against HSA and TFEB, in conjunction with the diverse characteristics of VNARs, we proposed a rational strategy for screening naïve and antigen-immunized libraries. Depending on the nature of antigens such as sequence conservation and *in vivo* exposure, an appropriate approach could be selected. For screening with naïve libraries, prioritizing VNAR1 and VNAR2 will enhance "hit" rates and increase the diversity of identified nanobodies. Our results provide a practical template for the research and development of therapeutic and diagnostic applications based on shark VNARs.

Acknowledgements

We are indebted to Wenxiang Zhao, Zhengbing Lyu, Yuchao Gu, Tianlei Ying and Yang Li for scientific advice; to Tingting Ning, Yanan Wang, Peng Xu, Zhongqiu Wu, Shitao Feng, Qiumei Zhu, Xiaofeng Jiang, Yanwen Guo, Bo Zhong, Ling Sun and Qiujie Yang for technical assistance; and to Zhiwei Huang, Zhenyu Wang, Zemin Bai and Lei Zhao for logistic support. This work is supported by research grants from Sanya Yazhou Bay Science & Technology City Administration (SKJC-2022-01-002 to Ming-Wei Wang and SKJC-2024-03-001 to Hao Li, China) and Special Project for the Promotion of Deep-Sea Technology Industry, Hainan Deep-Sea Technology Innovation Center (DSTIC-CYCJ-2023012 to Ming-Wei Wang, China).

Author contributions

Hao Li, Litong Liu, Xinyi Kang, Chuan-Wei Chen, Mengran Wang and Shaoqin Fu performed research; Bo Zhao and Dehua Yang assisted in study planning; Hao Li, Litong Liu, Xinyi Kang, Chuan-Wei Chen, Mengran Wang, Qingtong Zhou and Ming-Wei Wang analyzed the data and wrote the manuscript with inputs from all co-authors; Ming-Wei Wang initiated the project and supervised the studies.

Conflicts of interest

All the authors declare no conflicts of interest.

Appendix A. Supporting information

Supporting information to this article can be found online at https://doi.org/10.1016/j.apsb.2025.02.012.

References

1. Strohl WR. Structure and function of therapeutic antibodies approved by the US FDA in 2023. *Antib Ther* 2024;**7**:132−56.
2. Paul S, Konig MF, Pardoll DM, Bettegowda C, Papadopoulos N, Wright KM, et al. Cancer therapy with antibodies. *Nat Rev Cancer* 2024;**24**:399−426.
3. Bannas P, Hambach J, Koch-Nolte F. Nanobodies and nanobody-based human heavy chain antibodies as antitumor therapeutics. *Front Immunol* 2017;**8**:1603.
4. Iezzi ME, Policastro L, Werbajh S, Podhajcer O, Canziani GA. Single-domain antibodies and the promise of modular targeting in cancer imaging and treatment. *Front Immunol* 2018;**9**:273.
5. Wang M, Ying T, Wu Y. Single-domain antibodies as therapeutics for solid tumor treatment. *Acta Pharm Sin B* 2024;**14**:2854−68.
6. Fan Y, Feng R, Zhang X, Wang ZL, Xiong F, Zhang S, et al. Encoding and display technologies for combinatorial libraries in drug discovery: the coming of age from biology to therapy. *Acta Pharm Sin B* 2024;**14**: 3362−84.
7. Li C, Zhan W, Yang Z, Tu C, Hu G, Zhang X, et al. Broad neutralization of SARS-CoV-2 variants by an inhalable bispecific single-domain antibody. *Cell* 2022;**185**:1389−401.e18.
8. Stocki P, Szary J, Rasmussen CLM, Demydchuk M, Northall L, Logan DB, et al. Blood−brain barrier transport using a high affinity, brain-selective VNAR antibody targeting transferrin receptor 1. *FASEB J* 2021;**35**:e21172.
9. Li T, Vandesquille M, Koukouli F, Dudeffant C, Youssef I, Lenormand P, et al. Camelid single-domain antibodies: a versatile tool for *in vivo* imaging of extracellular and intracellular brain targets. *J Control Release* 2016;**243**:1−10.
10. Nie J, Ma X, Hu F, Miao H, Feng X, Zhang P, et al. Designing and constructing a phage display synthesized single domain antibodies library based on camel VHHs frame for screening and identifying humanized TNF-α-specific nanobody. *Biomed Pharmacother* 2021; **137**:111328.
11. Camacho-Villegas T, Mata-González M, García-Ubbelohd W, Núñez-García L, Elosua C, Paniagua-Solis J, et al. Intraocular Penetration of a vNAR: *in vivo* and *in vitro* VEGF165 neutralization. *Mar Drugs* 2018;**16**:113.
12. Xi X, Wang Y, An G, Feng S, Zhu Q, Wu Z, et al. A novel shark VNAR antibody-based immunotoxin targeting TROP-2 for cancer therapy. *Acta Pharm Sin B* 2024;**14**:4806−18.
13. Hamers-Casterman C, Atarhouch T, Muyldermans S, Robinson G, Hamers C, Songa EB, et al. Naturally occurring antibodies devoid of light chains. *Nature* 1993;**363**:446−8.
14. Greenberg AS, Avila D, Hughes M, Hughes A, McKinney EC, Flajnik MF. A new antigen receptor gene family that undergoes rearrangement and extensive somatic diversification in sharks. *Nature* 1995;**374**:168−73.
15. Leach A, Smyth P, Ferguson L, Steven J, Greene MK, Branco CM, et al. Anti-DLL4 VNAR targeted nanoparticles for targeting of both tumour and tumour associated vasculature. *Nanoscale* 2020;**12**: 14751−63.
16. Wu Y, Jiang S, Ying T. Single-domain antibodies as therapeutics against human viral diseases. *Front Immunol* 2017;**8**:1802.
17. Feige MJ, Grawert MA, Marcinowski M, Hennig J, Behnke J, Auslander D, et al. The structural analysis of shark IgNAR antibodies reveals evolutionary principles of immunoglobulins. *Proc Natl Acad Sci U S A* 2014;**111**:8155−60.
18. Stanfield RL, Dooley H, Flajnik MF, Wilson IA. Crystal structure of a shark single-domain antibody V region in complex with lysozyme. *Science* 2004;**305**:1770−3.
19. Streltsov VA, Varghese JN, Carmichael JA, Irving RA, Hudson PJ, Nuttall SD. Structural evidence for evolution of shark Ig new antigen receptor variable domain antibodies from a cell-surface receptor. *Proc Natl Acad Sci U S A* 2004;**101**:12444−9.
20. Leow CH, Fischer K, Leow CY, Braet K, Cheng Q, McCarthy J. Isolation and characterization of malaria PfHRP2 specific V(NAR) antibody fragments from immunized shark phage display library. *Malar J* 2018;**17**:383.
21. Dooley H, Flajnik MF. Antibody repertoire development in cartilaginous fish. *Dev Comp Immunol* 2006;**30**:43−56.
22. Johnson WE. Camelid genetics and reproductive biotechnologies. *J Hered* 2014;**105**:837−8.
23. Jiang X, Sun L, Hu C, Zheng F, Lyu Z, Shao J. Shark IgNAR: the next broad application antibody in clinical diagnoses and tumor therapies?. *Mar Drugs* 2023;**21**:496.
24. Wei L, Wang M, Xiang H, Jiang Y, Gong J, Su D, et al. Bamboo shark as a small animal model for single domain antibody production. *Front Bioeng Biotechnol* 2021;**9**:792111.
25. Sabir JSM, Atef A, El-Domyati FM, Edris S, Hajrah N, Alzohairy AM, et al. Construction of naïve camelids VHH repertoire in phage display-based library. *Comptes Rendus Biologies* 2014;**337**: 244−9.
26. Zhao P, Zhang Y, Li W, Jeanty C, Xiang G, Dong Y. Recent advances of antibody drug conjugates for clinical applications. *Acta Pharm Sin B* 2020;**10**:1589−600.
27. Chen WH, Hajduczki A, Martinez EJ, Bai H, Matz H, Hill TM, et al. Shark nanobodies with potent SARS-CoV-2 neutralizing activity and broad sarbecovirus reactivity. *Nat Commun* 2023;**14**:580.
28. Muller MR, Saunders K, Grace C, Jin M, Piche-Nicholas N, Steven J, et al. Improving the pharmacokinetic properties of biologics by fusion to an anti-HSA shark VNAR domain. *mAbs* 2012;**4**:673−85.
29. Muller MR, O'Dwyer R, Kovaleva M, Rudkin F, Dooley H, Barelle CJ. Generation and isolation of target-specific single-domain

antibodies from shark immune repertoires. *Methods Mol Biol* 2012;**907**: 177−94.
30. Jia L, Wang Y, Shen Y, Zhong B, Luo Z, Yang J, et al. IgNAR characterization and gene loci identification in whitespotted bamboo shark (*Chiloscyllium plagiosum*) genome. *Fish Shellfish Immunol* 2023;**133**:108535.
31. Wu Y, Li C, Xia S, Tian X, Kong Y, Wang Z, et al. Identification of human single-domain antibodies against SARS-CoV-2. *Cell Host Microbe* 2020;**27**:891−8.e5.
32. Li W, Chen M, Wang T, Feng X, Jiang X, Dong X, et al. Characterization and humanization of VNARs targeting human serum albumin from the whitespotted bamboo shark (*Chiloscyllium plagiosum*). *Int J Biol Macromol* 2024;**273**:133082.
33. Sullivan CJ, Pendleton ED, Sasmor HH, Hicks WL, Farnum JB, Muto M, et al. A cell-free expression and purification process for rapid production of protein biologics. *Biotechnol J* 2016;**11**:238−48.
34. Liu X, Wang Y, Sun L, Xiao G, Hou N, Chen J, et al. Screening and optimization of shark nanobodies against SARS-CoV-2 spike RBD. *Antivir Res* 2024;**226**:105898.
35. van Faassen H, Ryan S, Henry KA, Raphael S, Yang Q, Rossotti MA, et al. Serum albumin-binding V_H Hs with variable pH sensitivities enable tailored half-life extension of biologics. *FASEB J* 2020;**34**:8155−71.
36. Zorzi A, Linciano S, Angelini A. Non-covalent albumin-binding ligands for extending the circulating half-life of small biotherapeutics. *Medchemcomm* 2019;**10**:1068−81.
37. Wilkin TJ, Schoenfeld SL, Diaz JL, Kruse V, Bonifacio E, Palmer JP. Systematic variation and differences in insulin-autoantibody measurements. *Diabetes* 1989;**38**:172−81.
38. Li Y, Xu M, Ding X, Yan C, Song Z, Chen L, et al. Protein kinase C controls lysosome biogenesis independently of mTORC1. *Nat Cell Biol* 2016;**18**:1065−77.
39. Nanobodies Muyldermans S. Natural single-domain antibodies. *Annu Rev Biochem* 2013;**82**:775−97.
40. Liu JL, Shriver-Lake LC, Anderson GP, Zabetakis D, Goldman ER. Selection, characterization, and thermal stabilization of llama single domain antibodies towards Ebola virus glycoprotein. *Microb Cell Factories* 2017;**16**:223.
41. Lai JY, Lim TS. Infectious disease antibodies for biomedical applications: a mini review of immune antibody phage library repertoire. *Int J Biol Macromol* 2020;**163**:640−8.
42. Silacci M, Brack S, Schirru G, Mårlind J, Ettorre A, Merlo A, et al. Design, construction, and characterization of a large synthetic human antibody phage display library. *Proteomics* 2005;**5**:2340−50.
43. Farasat A, Rahbarizadeh F, Hosseinzadeh G, Sajjadi S, Kamali M, Keihan AH. Affinity enhancement of nanobody binding to EGFR: *in silico* site-directed mutagenesis and molecular dynamics simulation approaches. *J Biomol Struct Dyn* 2016;**35**:1710−28.
44. Muyldermans S. A guide to: generation and design of nanobodies. *FEBS J* 2020;**288**:2084−102.
45. Tanaka Y, Nishikawa M, Kamisaki K, Hachiya S, Nakamura M, Kuwazuru T, et al. Marine-derived microbes and molecules for drug discovery. *Inflamm Regen* 2022;**42**:18.
46. Takezaki N, Figueroa F, Zaleska-Rutczynska Z, Klein J. Molecular phylogeny of early vertebrates: monophyly of the agnathans as revealed by sequences of 35 genes. *Mol Biol Evol* 2003;**20**: 287−92.
47. Flajnik MF. A cold-blooded view of adaptive immunity. *Nat Rev Immunol* 2018;**18**:438−53.
48. Ma GJ, Ferhan AR, Sut TN, Jackman JA, Cho NJ. Understanding how natural sequence variation in serum albumin proteins affects conformational stability and protein adsorption. *Colloids Surf B Biointerfaces* 2020;**194**:111194.
49. Barelle C, Gill DS, Charlton K. Shark novel antigen receptors—the next generation of biologic therapeutics?. *Adv Exp Med Biol* 2009; **655**:49−62.
50. Dooley H, Flajnik MF, Porter AJ. Selection and characterization of naturally occurring single-domain (IgNAR) antibody fragments from immunized sharks by phage display. *Mol Immunol* 2003;**40**: 25−33.
51. Dooley H, Stanfield RL, Brady RA, Flajnik MF. First molecular and biochemical analysis of *in vivo* affinity maturation in an ectothermic vertebrate. *Proc Natl Acad Sci U S A* 2006;**103**:1846−51.
52. Nuttall SD, Walsh RB. Display scaffolds: protein engineering for novel therapeutics. *Curr Opin Pharmacol* 2008;**8**:609−15.
53. Tsuchiya Y, Mizuguchi K. The diversity of H3 loops determines the antigen-binding tendencies of antibody CDR loops. *Protein Sci* 2016; **25**:815−25.
54. D'Angelo S, Ferrara F, Naranjo L, Erasmus MF, Hraber P, Bradbury ARM. Many routes to an antibody heavy-chain CDR3: necessary, yet insufficient, for specific binding. *Front Immunol* 2018;**9**: 395.
55. Kuroda D, Tsumoto K. Structural classification of CDR-H3 in single-domain V_HH antibodies. *Methods Mol Biol* 2023;**2552**:61−79.
56. Truong TTT, Huynh VQ, Vo NT, Nguyen HD. Studying the characteristics of nanobody CDR regions based on sequence analysis in combination with 3D structures. *J Genet Eng Biotechnol* 2022;**20**:157.
57. DeKosky BJ, Lungu OI, Park D, Johnson EL, Charab W, Chrysostomou C, et al. Large-scale sequence and structural comparisons of human naive and antigen-experienced antibody repertoires. *Proc Natl Acad Sci U S A* 2016;**113**:E2636−45.
58. Mendoza MN, Jian M, King MT, Brooks CL. Role of a noncanonical disulfide bond in the stability, affinity, and flexibility of a VHH specific for the Listeria virulence factor InlB. *Protein Sci* 2020; **29**:1004−17.
59. Kovalenko OV, Olland A, Piche-Nicholas N, Godbole A, King D, Svenson K, et al. Atypical antigen recognition mode of a shark immunoglobulin new antigen receptor (IgNAR) variable domain characterized by humanization and structural analysis. *J Biol Chem* 2013;**288**:17408−19.
60. Feng M, Bian H, Wu X, Fu T, Fu Y, Hong J, et al. Construction and next-generation sequencing analysis of a large phage-displayed V_{NAR} single-domain antibody library from six naive nurse sharks. *Antib Ther* 2019;**2**:1−11.
61. Muyldermans S, Baral TN, Retamozzo VC, De Baetselier P, De Genst E, Kinne J, et al. Camelid immunoglobulins and nanobody technology. *Vet Immunol Immunopathol* 2009;**128**:178−83.
62. Liu JL, Anderson GP, Delehanty JB, Baumann R, Hayhurst A, Goldman ER. Selection of cholera toxin specific IgNAR single-domain antibodies from a naive shark library. *Mol Immunol* 2007; **44**:1775−83.
63. Miklos K, Tolnay M, Bazin H, Medgyesi GA. Rat IgG subclasses mediating binding and phagocytosis of target cells by homologous macrophages. *Mol Immunol* 1993;**30**:1273−8.
64. Hanson QM, Barb AW. A perspective on the structure and receptor binding properties of immunoglobulin G Fc. *Biochemistry* 2015;**54**: 2931−42.